Molecular Therapy
Original Article

KLF16 enhances stress tolerance of colorectal carcinomas by modulating nucleolar homeostasis and translational reprogramming

Xiao-Dan Ma,[1,7] Shui-Dan Xu,[1,7] Shi-Hui Hao,[2,7] Kai Han,[3] Jie-Wei Chen,[1,4] Han Ling,[1] Ri-Xin Chen,[5] Xiao-Han Jin,[6] Jing-Hua Cao,[1] Jin-Long Lin,[1] Qing-Jian Ou,[3] Yu-Jing Fang,[3] Zhi-Zhong Pan,[3] Dan Xie,[1,4] and Feng-Wei Wang[1]

[1]Sun Yat-sen University Cancer Center, State Key Laboratory of Oncology in South China, Collaborative Innovation Center for Cancer Medicine, No. 651 Dongfeng Road East, Guangzhou 510060, China; [2]Department of Nuclear Medicine, Sun Yat-sen University Cancer Center, State Key Laboratory of Oncology in South China, Collaborative Innovation Center for Cancer Medicine, Guangzhou 510060, China; [3]Department of Colorectal Surgery, Sun Yat-sen University Cancer Center, State Key Laboratory of Oncology in South China, Collaborative Innovation Center for Cancer Medicine, Guangzhou 510060, China; [4]Department of Pathology, Sun Yat-sen University Cancer Center, State Key Laboratory of Oncology in South China, Collaborative Innovation Center for Cancer Medicine, No. 651 Dongfeng Road East, Guangzhou 510060, China; [5]Department of Thoracic Surgery, Guangdong Provincial People's Hospital, Guangdong Academy of Medical Sciences, Guangzhou 510080, China; [6]Department of Urology, First Affiliated Hospital, Sun Yat-sen University, Guangzhou 510080, China

Translational reprogramming is part of the unfolded protein response (UPR) during endoplasmic reticulum (ER) stress, which acts to the advantage of cancer growth and development in different stress conditions, but the mechanism of ER stress-related translational reprogramming in colorectal carcinoma (CRC) progression remains unclear. Here, we identified that Krüppel-like factor 16 (KLF16) can promote CRC progression and stress tolerance through translational reprogramming. The expression of KLF16 was upregulated in CRC tissues and associated with poor prognosis for CRC patients. We found that ER stress inducers can recruit KLF16 to the nucleolus and increase its interaction with two essential proteins for nucleolar homeostasis: nucleophosmin1 (NPM1) and fibrillarin (FBL). Moreover, knockdown of KLF16 can dysregulate nucleolar homeostasis in CRC cells. Translation-reporter system and polysome profiling assays further showed that KLF16 can effectively promote cap-independent translation of ATF4, which can enhance ER-phagy and the proliferation of CRC cells. Overall, our study unveils a previously unrecognized role for KLF16 as an ER stress regulator through mediating translational reprogramming to enhance the stress tolerance of CRC cells and provides a potential therapeutic vulnerability.

INTRODUCTION

The endoplasmic reticulum (ER) is an essential organelle for protein homeostasis (proteostasis). ER stress is caused by intracellular or extracellular stress, such as hypoxia, nutrient deprivation, oxidative stress, low pH, and high metabolic demand. Stresses disturb the protein folding capacity of the ER, and in response, cells elicit an unfolded protein response (UPR) to restore proteostasis.[1] Binding-immunoglobulin protein (BIP) functions as a master regulator of the UPR. During ER stress, BIP is sequestered by unfolded proteins and thus activates three ER stress sensors: protein kinase RNA (PKR)-like ER kinase (PERK), inositol requiring enzyme1 (IRE1), and activating transcription factor 6 (ATF6).[2] These sensors alter both transcriptional and translational programs in stressed cells. PERK signaling initiates an immediate adaptive translation regulation by phosphorylating eukaryotic translation initiation factor 2 subunit-α (eIF2α), which reduces protein synthesis by restricting 5′ cap-dependent translation.[3,4] Concomitantly, a set of UPR-related proteins translates in a cap-independent mode, including ATF4.[5] ATF4 subsequently induces the expression of a variety of cytoprotective genes acting in particular on amino acid metabolism, oxidative stress damage, and ER-phagy.[1,6] IRE1-XBP1s and ATF6 pathways also affect almost every step of protein turnover, which includes protein folding, trafficking, and degradation.[7] When the UPR is insufficient for the proteostasis, the cell will undergo terminal UPR, culminating in cell death.[8]

The deregulation of stress response pathways plays a central role in cancer initiation and malignant expansion, because cancer cells must balance high metabolic demands for proliferation and nutrient deficiency in the new environment.[9] This hostile living condition provokes a sustained UPR, which can make cancer cells more

Received 7 November 2021; accepted 29 April 2022;
https://doi.org/10.1016/j.ymthe.2022.04.022.

[7]These authors contributed equally

Correspondence: Feng-Wei Wang, M.D., State Key Laboratory of Oncology in South China, Sun Yat-sen University Cancer Center, No. 651, Dongfeng Road East, Guangzhou 510060, China.
E-mail: wangfengw@sysucc.org.cn
Correspondence: Dan Xie, M.D.State Key Laboratory of Oncology in South China, Sun Yat-sen University Cancer Center, No. 651, Dongfeng Road East, Guangzhou 510060, China.
E-mail: xiedan@sysucc.org.cn

tumorigenic, highly aggressive, and drug resistant.[1,2] Colorectal carcinoma (CRC) is ranked as the third most common cancer worldwide.[10] Great efforts have been dedicated to understanding the relationship between ER stress and the carcinogenesis and progression of CRC.[11] For instance, ATF4 upregulates RNASET2-mediated uracil generation, which impairs exogenous 5-fluorouracil (5-FU) uptake and leads to decreased 5-FU therapeutic sensitivity in CRC.[12] Specific expression of the active form of ATF6 in intestinal epithelial cells of mice promotes dysbiosis and microbiota-dependent tumorigenesis.[13] Moreover, multiple studies have shown that the inhibition of the UPR decelerates cancer growth.[14–16] You et al. identified potential genes involved in regulating UPR through a genome-wide CRISPR screen in the CRC cell line HT-29.[8] However, the underlying mechanism of pro-tumorigenic UPR in CRC remains unknown.

Krüppel-like factors (KLFs) belong to the family of zinc finger-containing TFs. Approximately 17 members of the KLF family have been identified, and most of them are involved in embryogenesis, development, and homeostasis, as well as carcinogenesis and cancer progression.[17] One of the best-known members is KLF4, which can reprogram somatic cells into induced pluripotent stem cells (iPSCs) together with three other TFs.[18] Numerous studies have reported that KLFs serve as tumor suppressors or oncogenes depending on the specific cellular context. Deletion of KLF4 inhibits the localization of p53 to the centrosome in mouse embryonic fibroblasts (MEFs) and induces more colon adenomatous polyps and carcinomas *in situ* in mouse models.[19] KLF5 is an independent prognostic factor for CRC and plays a critical role in regulating cancer stemness by increasing the expression of cyclin D1 and c-MYC.[20,21] KLF16 is involved in the metabolism and regulation of the endocrine system and plays different roles in different cancers.[22–25] A hepatic KLF16 knockout mouse model revealed that KLF16 closely links hepatic lipid homeostasis and redox balance by regulating the transcriptional activity of peroxisome proliferator-activated receptor alpha (PPARα).[22] Perturbation of cellular redox status is one of the causes of ER stress.[26] However, whether the KLF family can regulate UPR in cancer remains unknown.

By screening databases and the literature concerning the UPR in CRC, we identify KLF16 as a potential UPR regulator in CRC pathogenesis. In this study, we highlight a new role for nucleolar KLF16 in programming cap-independent translation by interacting with essential nucleolar proteins nucleophosmin1 (NPM1) and fibrillarin (FBL), and consequently, enhancing cellular stress tolerance and pathogenesis of CRC.

RESULTS

KLF16 is upregulated in CRC and related to UPR

To screen potential KLF family members related to CRC carcinogenesis, we assessed the expression of KLFs between 41 pairs of CRC tumors and their paracancerous tissues in The Cancer Genome Atlas (TCGA) database. We found that KLF1, KLF7, and KLF16 are significantly upregulated and that most of the other members are significantly downregulated in CRC (Figure S1A). You et al. performed a genome-scale screen in CRC cell line HT-29 to identify the regulators of the UPR pathway.[8] By comparing KLFs with hits from the UPR-related CRISPR screen, we found that KLF5, KLF8, and KLF16 were listed as potential genes regulating the UPR[8] (Figure S1B). Combining these two results, we focused on KLF16, which is upregulated in CRC cancer tissues and may be an important oncogene for the pathogenesis of CRC.

To investigate whether KLF16 is involved in the UPR, we initially examined the expression levels of several ER stress markers after KLF16 knockdown or overexpression. Stress was induced using the ER stress inducer, thapsigargin (Tg). In agreement with our hypothesis, the UPR was significantly attenuated by KLF16 knockdown and enhanced by KLF16 overexpression (Figures 1A and S2A). After treatment with Tg or another ER stress-inducing agent, tunicamycin (Tm), we found that KLF16 knockdown also reduced the tolerance of CRC cells against ER stress (Figures 1B and S2B). Although there was no significant proliferative difference between siKLF16 cells and control cells in normal culture conditions (Figures S2C and S2D), KLF16 knockdown suppressed the proliferation (Figures S2C and S2D) and the expression of ER stress markers (Figure S2E) under serum-starvation and glucose-starvation conditions in CRC cells. Moreover, the UPR inhibitor GSK2606414 could attenuate the effects of KLF16 on cellular proliferation in glucose-starvation conditions (Figure S2F). These data collectively implied that KLF16 promotes cell proliferation in CRC by regulating the UPR. In addition, we examined the expression of KLF16 in CRC tissues. As shown in Figures 1C–1E, compared with matched paracancerous tissues, both the mRNA and protein expression levels of KLF16 were dramatically higher in CRC tissues. Correlation analysis demonstrated that the high expression of KLF16 was positively correlated with aggressive clinicopathological characteristics (Table S1). Meanwhile, Kaplan-Meier analysis showed that CRC patients with higher levels of KLF16 expression had shorter survival (Figure 1F), and KLF16 was proved to be an independent predictor using Cox regression analysis (Table S2).

KLF16 interacts with the nucleolar proteins NPM1 and FBL

To gain molecular insight, we next performed anti-KLF16 immunoprecipitation (IP) assays followed by liquid chromatography-tandem mass spectrometry (LC-MS/MS) analysis. The enrichment analysis of LC-MS/MS results (accession number: IPX0004 454000) suggested that KLF16 coprecipitated with many proteins associated with ribosome biogenesis in eukaryotes. It is worth noting that, of the 286 genes required for pre-rRNA processing in the nucleolus,[27] 14 were identified in the KLF16 LC-MS/MS dataset (Figure S3A). Of particular interest are NPM1 and FBL, which are regarded as markers and essential regulators of the nucleolus.[28]

IP assays verified that KLF16 can interact with NPM1 and FBL (Figures 2A and 2B). We further examined the subcellular localization of KLF16 by immunofluorescence (IF) and observed that ER stress induced an accumulation of endogenous KLF16 in nucleoli and increased colocalization between KLF16 and either NPM1 or FBL in SW480 cells (Figures 2C and 2D). Both NPM1 and FBL are

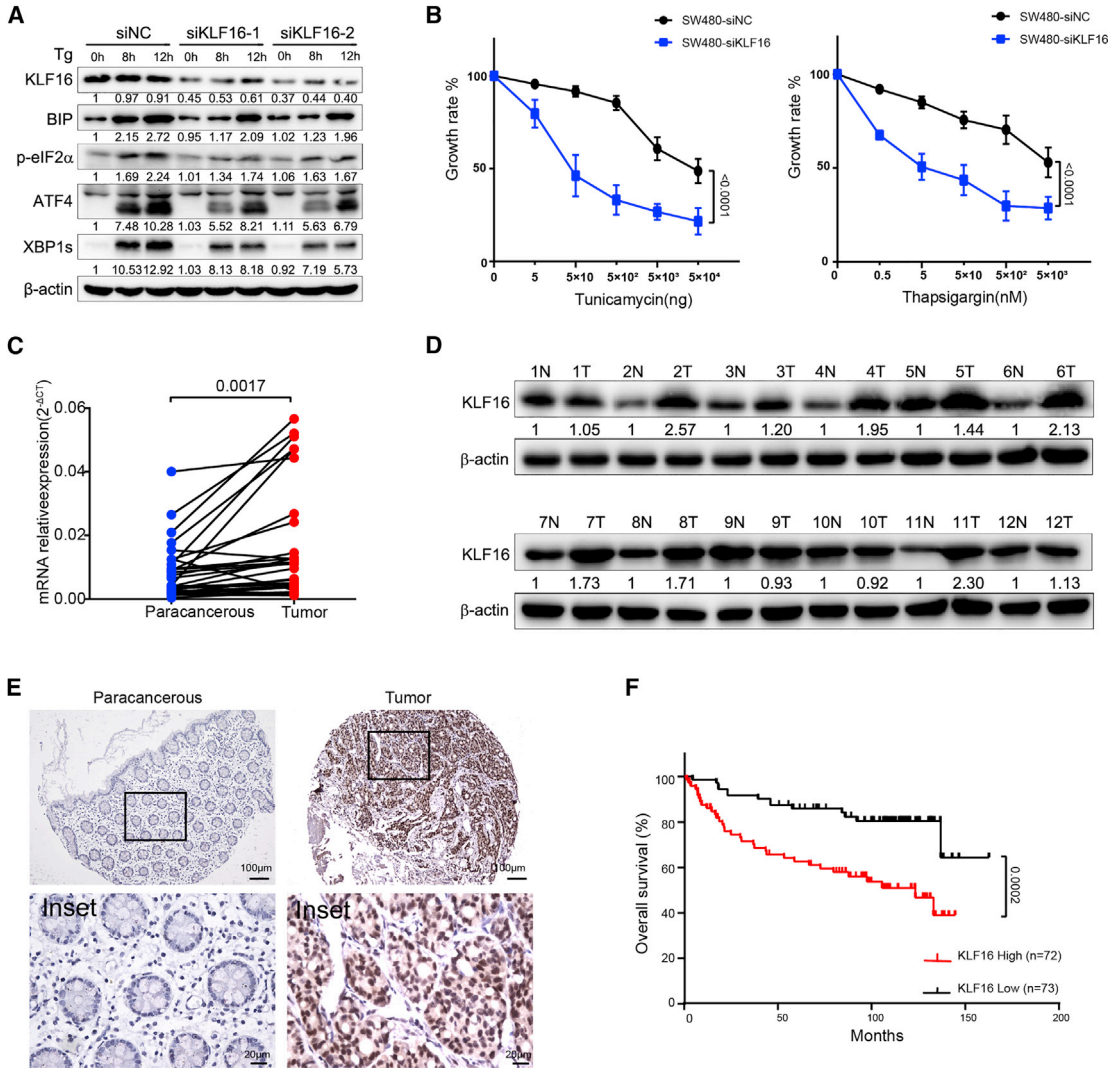

Figure 1. KLF16 regulates UPR activity and its expression in CRC

(A) KLF16 expression was knocked down by specific siRNA. After 48 h of the transfection, siNC and siKLF16 SW480 cells were treated with 100 nM thapsigargin (Tg) for the indicated time points, followed by western blotting (WB) assays, with β-actin as loading control. (B) KLF16 expression was knocked down by specific siRNA. After 24 h of the transfection, siNC and siKLF16 SW480 cells were treated with tunicamycin (0, 5, 5 × 10, 5×10^2, 5×10^3, and 5 × 10^4 ng) or Tg (0, 5 × 10^{-1}, 5, 5 × 10, 5×10^2, and 5 × 10^3 nM) for 72 h, and the cell growth rate was tested by the CCK-8 assay. Data represent the mean ± SD from n = 3 biologically independent experiments. Statistical significance was determined by a 2-way ANOVA. (C) Quantitative real-time-PCR analysis of *KLF16* mRNA expression in 30 CRC tissues and matched paracancerous tissues. Statistical significance was determined by a 2-tailed paired Student's t test. (D) WB assays of KLF16 protein expression in 12 CRC tissues and matched paracancerous tissues. β-Actin was used as loading control. (E) Representative IHC staining for KLF16 in CRC tissues and matched paracancerous tissues. Scale bar, 100 μm (20 μm for insets). (F) Kaplan-Meier analysis of OS in patients with stages II to III CRC with low versus high expression of KLF16 protein from SYSUCC cohorts (n = 145). Statistical significance was determined by a log rank test.

upregulated in CRC based on the GEPIA database (Figure S3B). Moreover, knockdown NPM1 or FBL can significantly reduce the proliferation of CRC cells (Figure S3C), which further supports a role for NPM1/FBL in the biological function of KLF16 in CRC.

To explore the relationships between KLF16/NPM1/FBL, we silenced NPM1 or FBL with small interfering RNA (siRNA). NPM1 knockdown significantly attenuated the interaction between KLF16 and FBL, whereas FBL knockdown had little effect on the interaction between KLF16 and NPM1 (Figure 2E). Moreover, NPM1 knockdown significantly decreased the nucleolar localization of KLF16 (Figure S3D). The translocation of KLF16 was also observed in the presence of BMH21, an inhibitor of ribosome biogenesis that also triggers the translocation of NPM1 into the nucleoplasm[29] (Figure S3D). These data suggest that NPM1 is necessary for the formation of the KLF16/NPM1/FBL complex.

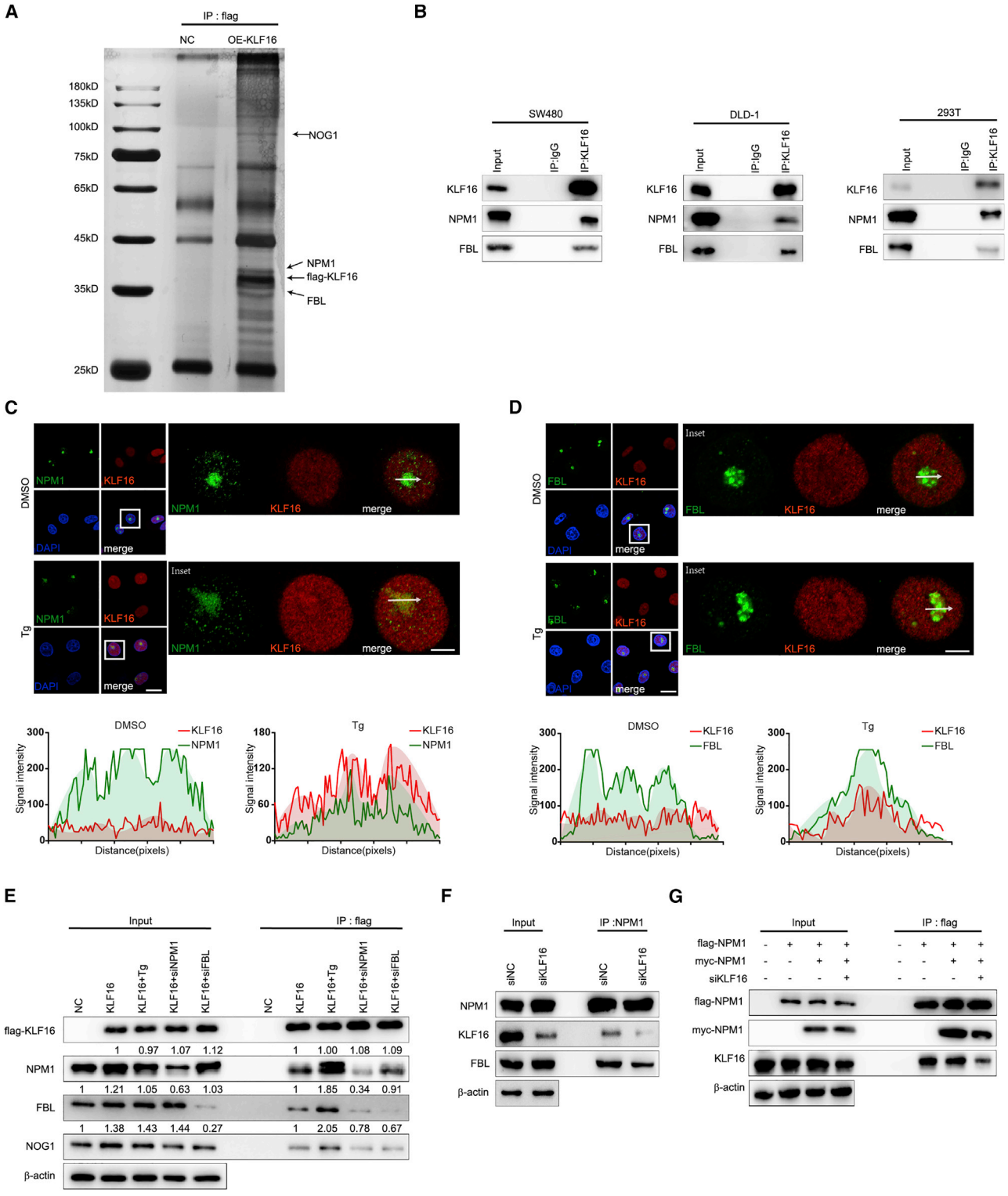

Figure 2. KLF16 interacts with NPM1 and FBL

(A) FLAG-KLF16 overexpression plasmids (OE-KLF16) and normal controlled plasmids (NC) were transfected into 293T cells. After 48 h of the transfection, cells were subjected to IP assay. Silver staining was carried out after IP assays. The arrows indicate the additional band present in OE-KLF16 cell extracts. (B) Anti-KLF16 antibody was

(legend continued on next page)

Reciprocal IP of NPM1 revalidated the KLF16/NPM1/FBL interaction, and KLF16 knockdown significantly decreased the NPM1-FBL interaction (Figure 2F). The oligomerization of NPM1 is critical for its participation in rRNA synthesis, processing, and quality control.[30–32] We therefore conducted IP assays of exogenously expressed FLAG-tagged NPM1 and myc-tagged NPM1 and found that KLF16 knockdown disrupted NPM1 oligomerization (Figure 2G). Our data collectively revealed that KLF16 binds NPM1 and FBL in the nucleolus.

N-terminal oligomerization domain (NTD) of KLF16 is necessary to nucleolus-nucleoplasm shuttling of KLF16

There are three highly conserved Cys2-His2 zinc fingers (C2H2) in KLF family members that are recognized as DNA-binding domains.[17,33] The C2H2 domains are also involved in the nuclear localization of these proteins.[34,35] In contrast, the variable N-terminal domains can recruit differential cofactors and perform different biological functions.[24]

We constructed three deletion-mutant KLF16 plasmids (Figure 3A). As shown in Figure 3B, KLF16ΔC2H2 failed to bind with NPM1, whereas KLF16ΔCTD (C-terminal nucleic acid-binding domain) and KLF16ΔNTD could still bind NPM1 with much reduced affinity. It is worth noting that none of the fragments can bind with FBL. KLF16ΔC2H2 indeed did not localize to the nucleolus, while KLF16ΔNTD accumulated in the nucleolus compared with the full-length (FL) protein (Figure 3C). The result revealed that the NTD of KLF16 is important to nucleolus-nucleoplasm shuttling of KLF16. The formation of KLF16/NPM1/FBL complex depends on much more than only molecular localization of KLF16 as KLF16ΔNTD accumulated in the nucleolus but with lower affinity.

We next sought to determine which domain of NPM1 is vital for the formation of KLF16/NPM1/FBL complex. NPM1 possesses an NTD, an intrinsically disordered region (IDR), and a CTD[36–38] (Figure S4A). Truncated mutants of NPM1 were transfected into 293T cells for IP assays. Apart from NPM1ΔCTD, all truncated mutants and FL NPM1 could interact with KLF16 and FBL (Figure S4B). Only NPM1ΔCTD was unable to localize to the nucleolus (Figure S4C). These findings suggest that the CTD domain of NPM1 is essential for the formation of the KLF16/NPM1/FBL complex and NPM1 nucleolar localization.

KLF16ΔNTD accumulated in the nucleolus, but lost the ability of the KLF16/NPM1/FBL complex formulation. As NPM is reported to be nucleolus-nucleoplasm shuttling proteins,[39] we then tested the effect of KLF16ΔNTD overexpression on localization of NPM1 and FBL. IF microscopy showed that neither KLF16-OE (overexpression) nor KLF16ΔNTD-OE cells affect the localization of NPM1 and FBL (Figures S4C and S4D).

KLF16 modulates nucleolar homeostasis

The nucleolus is a central response hub for stress.[40] Various stresses can modify nucleolar size, shape, and protein subcellular location.[28,41] NPM1 is the most abundant protein in the nucleolus and is critical for fundamental nucleolar processes such as rRNA synthesis, rRNA modifications, and ribosome assembly, as well as nucleolar structure and stress response.[28,36,39,41,42] Therefore, we performed a series of experiments examining whether KLF16 affects nucleolar homeostasis. The main function of the nucleolus is rRNA production.[27] As shown in Figures 4A and 4B, similar to the result of NPM1 and FBL, knockdown of KLF16 decreased the rRNA production of nascent 47*S* rRNA and cytoplasmic mature rRNA expression levels. A 5-ethynyluridine (EU) labeling assay revealed that KLF16 knockdown suppressed nascent RNA synthesis in the nucleolus (Figure 4C). Furthermore, KLF16-altered nucleolar morphology resembles the effect of NPM1. KLF16 knockdown increased the frequency of cells with nucleolar abnormalities (Figure 4D). Consistently, Tg treatment-induced ER stress also affected nucleolar functions (Figures 4E and 4F). These results inform us that KLF16 regulates rDNA transcription. Interestingly, the promoter of rDNA is GC rich,[43,44] and GC-rich genomic regulatory regions serve as potential binding sites for KLFs.[24] Using a dual-luciferase reporter system of the rDNA promoter, we found that ER stress inhibited rDNA promoter activity, and that this effect was reversed by KLF16-OE (Figure 4G). Together, these experiments confirm the essential role of KLF16 in the nucleolar homeostasis of stressed cells.

KLF16 promotes cap-independent translation during ER stress

The nucleolus is the factory of ribosome biogenesis.[42] Dysregulation of nucleolar homeostasis affects ribosome biogenesis and results in translational reprogramming.[45–47] NPM1 and FBL regulate cap-independent translation by modulating rRNA 2′-*O*-Me modifications.[48–51] During ER stress, cap-dependent translation is inhibited by phosphorylated eIF2α and cap-independent translation activates concomitantly.[7] We thus proposed that KLF16 functions with NPM1 and FBL to modulate cap-independent translation during ER stress.

There are two upstream open reading frames in the 5′ untranslated region (5′UTR) of ATF4 that guarantee its upregulation during ER

used for endogenous IP assays in cell extracts from exponentially growing SW480, DLD-1, or 293T cells. Mouse immunoglobulin G (IgG) was used as a negative control. (C) Immunofluorescence (IF) staining of SW480 cells treated with DMSO or Tg and stained with anti-NPM1 (green) and anti-KLF16 (red) antibodies. DAPI staining shows nuclei. Line graphs represent signal intensity along the arrow bars for each protein. Scale bar, 20 μm (5 μm for insets). (D) IF staining of SW480 cells treated with DMSO or Tg and stained with anti-FBL (green) and anti-KLF16 (red) antibodies. DAPI staining shows nuclei. Line graphs represent signal intensity along the arrow bars for each protein. Scale bar, 20 μm (5 μm for insets). (E) OE-KLF16 and NC plasmids were transfected into 293T cells. After 48 h of the transfection, cells were subjected to IP assay followed by WB assays with the indicated antibodies. (F) Endogenous IP of NPM1 antibody in siNC and siKLF16 SW480 cells followed by WB assays with the indicated antibodies. (G) After 12h of the transfection with FLAG- and myc-tagged NPM1-expressing plasmids, 293T cells were transfected with siRNA. After 36 h of the transfection, cells subjected to IP assay of the exogenously expressed FLAG-NPM1 to show the interactions between NPM1 proteins in siNC and siKLF16 cells.

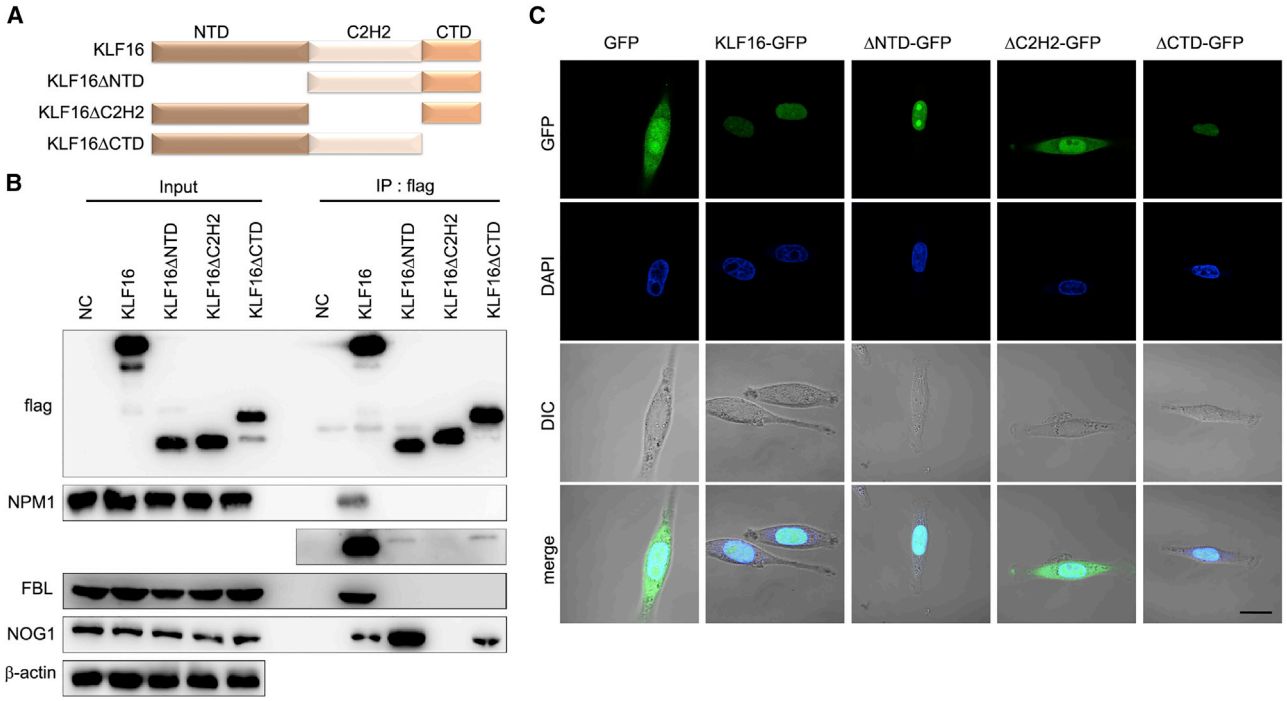

Figure 3. The role of KLF16 mutants in KLF16/NPM1/FBL complex

(A) Domain organization of the KLF16 protein and its truncated mutants. (B) KLF16 or KLF16-mutant plasmids were transfected into 293T cells. IP assays were carried out 48 h after transfection and followed by WB assays with the indicated antibodies. (C) Laser scanning confocal microscopy was used 48 h after transfection to monitor the distribution of GFP-tagged KLF16 with full-length or truncated mutants. Scale bar, 20 μm.

stress.[52] BIP and c-MYC are also reported to translate in a cap-independent manner through the internal ribosome entry site (IRES).[53] Therefore, we constructed a translation-reporter plasmid and inserted the 5′UTR of ATF4 as well as IRES elements of BIP or c-MYC to test their translational activity[50,51] (Figure 5A). Compared with the control group, the Fluc/Rluc ratio that reflects ATF4, BIP, and c-MYC translational activity was significantly decreased upon KLF16 knockdown during ER stress (Figures 5B, S5A, and S5B). Ectopic OE of NPM1 and FBL increased translational activities, and this effect was reversed by KLF16 knockdown (Figures 5C and S5C).

We then arranged time-dependent IRES-reporter assays and IP assays. In IRES-reporter assays, KLF16-knockdown affected the translational activity of CRC cells immediately (Figure S5D). NPM1/FBL/KLF16 complex formed within 30 min after cells were exposed to ER stress (Figure S5E). Together, these experiments provide some evidence to support the idea that KLF16 can regulate translation as soon as cells are exposed to ER stress.

Polysome profiling assays were performed to further validate the regulatory role of KLF16 on translational regulation. KLF16 knockdown resulted in a lower abundance of the mRNA of ATF4, BIP, and c-MYC in heavy polysome (HP) fractions, which indicates reduced translational activity (Figures 5D, 5E, S5G, and S5H). The distribution of those mRNAs was visualized by DNA agarose gel (Figures 5D, 5E, S5D, and S5E), and there was no significant change in cells cultured under normal conditions (Figure S6). These results strongly suggest that KLF16 enhanced cap-independent translational activity of target mRNAs during ER stress. Moreover, polysome profiling assays and puromycylation assays showed that KLF16 knockdown reduced global protein synthesis during ER stress (Figures 5F and 5G). Indeed, FBL or NPM knockdown reduced the protein level of ATF4, BIP, and c-MYC in stressed CRC cells (Figure 5H).

KLF16 increases stress tolerance of CRC by enhancing ATF4-dependent ER-phagy

To maintain cellular proteostasis in response to ER stress, cells emerge ER-phagy to recycle large amounts of misfolded proteins and membranous compartments.[54–58] To investigate whether KLF16 regulates ER-phagy, we next carried out an ER-phagy reporter assay. Using an ssRFP-GFP-KDEL plasmid, in which red fluorescent protein (RFP) and GFP fluorescence are detected in ER lumina but GFP fluorescence is quenched inside acidic lysosomes (Figure 6A),[58] we examined the ER-phagic flux by measuring the number of spots that showed only RFP fluorescence. KLF16 knockdown reduced the number of $RFP^{+}GFP^{-}$ spots, indicative of decreased ER-phagic flux during ER stress (Figure 6B).

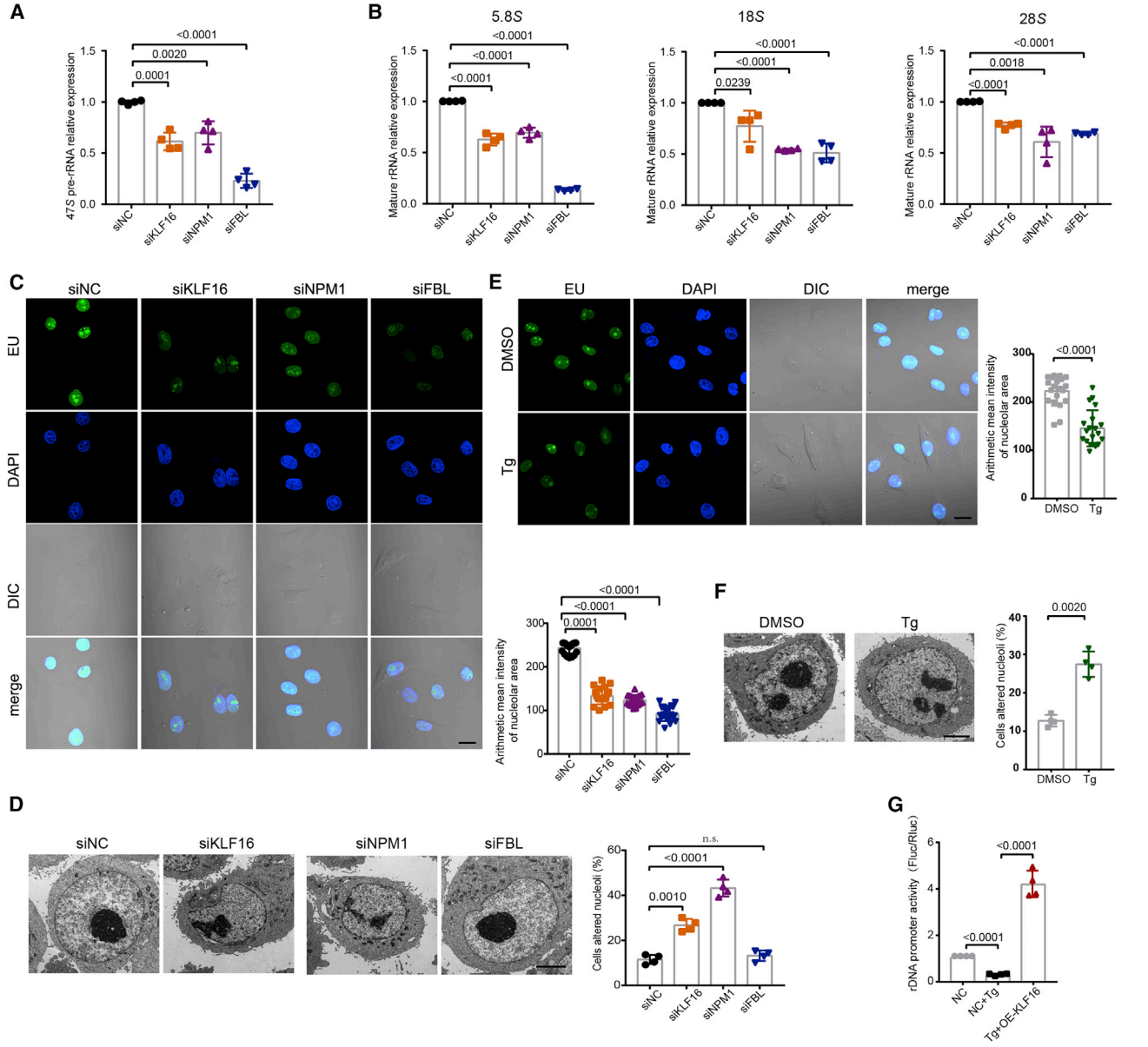

Figure 4. KLF16 can regulate nucleolar homeostasis

(A) The relative expression levels of the 47S pre-rRNAs were measured by quantitative real-time-PCR in SW480 cells transfected with the indicated siRNAs. β-Actin was used as a housekeeping gene for normalization. Data represent the mean ± SD from n = 4 biologically independent experiments. Statistical significance was determined by a two-tailed unpaired Student's t test. (B) The relative expression levels of the cytoplasmic rRNA were measured by quantitative real-time-PCR in SW480 cells transfected with the indicated siRNAs. β-Actin was used as a housekeeping gene for normalization. Data represent the mean ± SD from n = 4 biologically independent experiments. Statistical significance was determined by a two-tailed unpaired Student's t test. (C) SW480 cells transfected with the indicated siRNAs. After 36 h of the transfection, EU-labeled nascent RNA was evaluated by IF. DAPI staining shows nuclei. Scale bar, 20 μM. Arithmetic mean intensity of the nucleolar area of EU staining was calculated from 20 randomly selected cells for each group. Statistical significance was determined by a 2-tailed unpaired Student's t test. (D) Representative transmission electron micrographs showing the nucleolus in SW480 cells transfected with the indicated siRNAs. Scale bar, 5 μM. Percentage of SW480 cells with altered nucleoli after transfection with the indicated siRNAs. Statistical significance was determined by a 2-tailed unpaired Student's t test. (E) EU-labeled nascent RNA was measured by IF in SW480 cells with or without Tg treatment. DAPI staining shows nuclei. Scale bar, 20 μM. Arithmetic mean intensity of the nucleolar area of EU staining was calculated from 20 randomly selected cells for each group. Statistical significance was determined by a 2-tailed unpaired Student's t test. (F) Representative transmission electron micrographs showing the nucleolus in SW480 cells treated with or without Tg. Scale bar, 5 μM. Percentage of SW480 cells with altered nucleoli with or without Tg treatment. Statistical significance was determined by a 2-tailed unpaired Student's t test. (G) Luciferase activity of human rDNA promoter was measured in NC and OE-KLF16 SW480 cells with or without Tg treatment. Statistical significance was determined by a 2-tailed unpaired Student's t test.

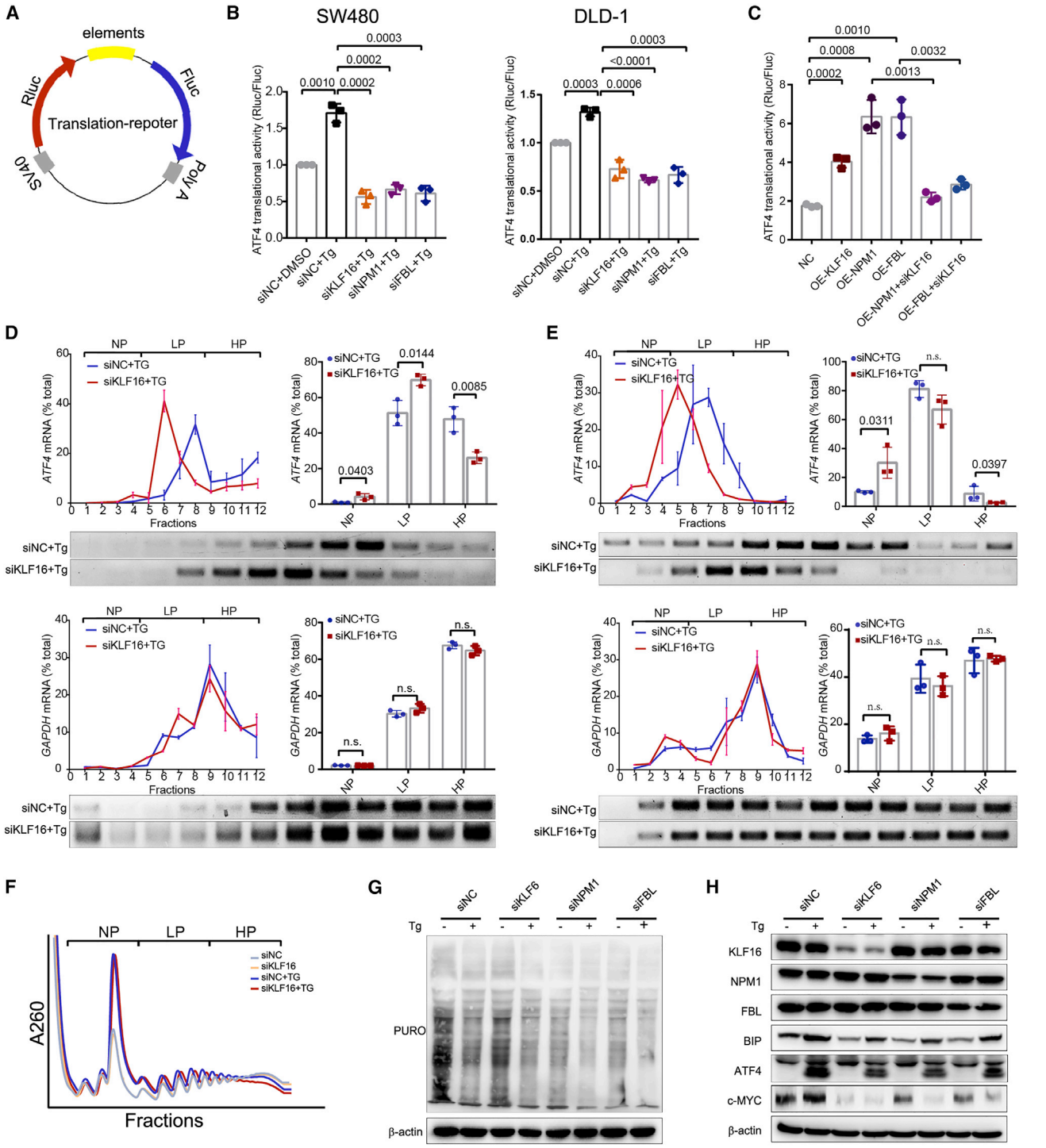

Figure 5. KLF16 regulates cap-independent translation activity of specific genes in the UPR

(A) Diagram of the translation-reporter plasmid testing cap-independent translation. (B) ATF4 translation-reporter plasmids were transfected into SW480 cells or DLD-1 cells. After 12 h of the first transfection, the indicated siRNAs were transfected. Cap-independent translation activity of ATF4 was measured 36 h after the second transfection by using dual-luciferase assays. Data represent the means ± SDs from n = 3 biologically independent experiments. Statistical significance was determined by a 2-tailed Student's t test. (C) ATF4 translation-reporter plasmids and OE plasmids were co-transfected into SW480. After 12 h of the first transfection, the indicated siRNAs were transfected. Then, cap-independent translation activity of ATF4 was measured 36 h after the second transfection by using dual-luciferase assays. Data represent the means ± SDs

(legend continued on next page)

ATF4 is essential for ER-phagy.[6] Moreover, upregulated ATF4 can promote CRC initiation, progression, and chemotherapy resistance.[59,60] We next assessed whether ATF4 mediates the biological function of KLF16. As shown in Figures 6C and 6D, ATF4 knockdown reversed the oncogenic effect of KLF16-OE.

We next determined whether NPM1 and FBL can regulate ER-phagy. ER-phagic flux assay was performed after silencing NPM1 or FBL. The results showed that NPM1 and FBL knockdown reduced the ER-phagic flux, which can be reversed by KLF16-OE (Figure 6E).

In addition, lentivirus-mediated stable knockdown of KLF16 greatly inhibited the growth of subcutaneous transplanted tumors in nude mice (Figure 7A), whereas its overexpression conferred a significant growth advantage to the transplanted tumors (Figure 7B). We detected the expression of ATF4 in xenograft tumor tissue samples and demonstrated that the expression of ATF4 was significantly increased in the KLF16-OEgroup (Figure 7C).

Finally, we measured the protein levels of KLF16 and ATF4 in cases of early-stage CRC by immunohistochemistry (IHC). Correlation analysis showed a positive correlation between KLF16 and ATF4 (Figures 7D and 7E). These data suggest that ATF4-mediated ER-phagy is critical for KLF16-driven carcinogenesis of CRC.

DISCUSSION

Growing evidence demonstrates the importance of translational reprogramming in carcinogenesis and cancer progression.[61] Stress inhibits cellular cap-dependent translation and cancer cells rely on alternating translation mode for the upregulation of stress-related genes to accommodate unremitting proliferation and maintain their competitive advantage.[5,62] In CRC, an integrated proteogenomic analysis illustrated that mRNA transcript abundance does not reliably predict protein abundance.[63] The research highlights the importance of translation steps in shaping the proteome of cancer cells. The current understanding of how KLF16 contributes to the malignant progression of cancers has focused on its ability to transcriptional regulation.[22,23,25] We show here that KLF16 also plays a critical role in translational regulation during ER stress. Mechanistically, KLF16 was recruited to the nucleolus during ER stress. By strengthening the interaction between NPM1 and FBL, KLF16 dysregulates nucleolar homeostasis and cap-independent translation of ATF4, BIP, and c-MYC, and thus enhances cellular stress tolerance of CRC cells. Our findings identify KLF16 as a key regulator of translational reprogramming, linking nucleolar homeostasis with ER stress.

Upstream signaling pathways, such as WNT, MAPK, and PI3K/AKT, play an important role in translational reprogramming in CRC,[61] but the contribution of ribosomes is relatively underappreciated. Our present work shows that KLF16 promotes rDNA transcription and knockdown KLF16 downregulates mature rRNA production and induces abnormal nucleolar morphology. Although we did not observe a significant change in cell proliferation under normal conditions after KLF16 knockdown, we noticed that the difference becomes appreciable under conditions that cause stress to cells and better mimic *in vivo* environments. Ribosome biogenesis is a major energy-consuming process and therefore it is well orchestrated but vulnerable to various stresses.[64] Some previous studies have suggested that UPR is interconnected with nucleolar homeostasis. PERK/p-eIF2α activation not only can inhibit Pol I activity activation but it can also increase free ribosomal proteins, which in turn regulate UPR and stress response in the nucleolus.[65–69] Here, we investigated the contribution of KLF16 in translational control and nucleolar homeostasis during ER stress, and established an unrecognized stress/KLF16/nucleolus/translation regulatory axis.

The exquisite manipulation of translational regulation reflects a powerful means for adaption in cancers.[70] Rapid technological advances have raised our understanding that the intrinsic translational control of ribosomes is modulated through rRNA modification.[49] Previous reports have proposed that NPM1 and FBL regulate cap-independent translation by modulating rRNA 2′-*O*-Me modifications[49,50] and that NPM1 is reported to recruit other partners into the nucleolus to facilitate nucleolar homeostasis.[36] While we do not define the precise mechanism, our data show that ER stress can induce KLF16 recruitment to the nucleolus, and therefore accumulation of the KLF16/NPM1/FBL complex in CRC cells and the transformation of translation mode. TF EZH2 is involved in cancer-related translational regulation via direct interaction with FBL.[51] Together with our findings, these reports exemplify a model in which TFs can modulate translational reprogramming by interacting with nucleolar proteins.

We constructed three mutants of KLF16, none of which could form the KLF16/NPM1/FBL complex. Since KLF16ΔNTD and KLF16ΔCTD still can be detected in the nucleolus, we speculate that the formation of the KLF16/NPM1/FBL complex is partly dependent on the nucleolar localization of KLF16. The KLF16ΔNTD mutant showed increased accumulation in the nucleolus compared to FL-KLF16. Clearly, further studies are needed to investigate the

from n = 3 biologically independent experiments. Statistical significance was determined by a 2-tailed unpaired Student's t test. (D and E) Polysome of the SW480 (D) and DLD-1 (E) cells with Tg treatment were extracted and subjected to a 10%–50% sucrose gradient by ultracentrifugation. Twelve polysome fractions were collected from top to bottom, followed by RNA extraction. *ATF4* and *GAPDH* mRNA expression in each fraction was determined by quantitative real-time-PCR (upper) and visualized by DNA agarose gel (lower). The relative amounts of non-polysome (fractions 1–4), light polysome (fractions 5–8), and heavy polysome (fractions 9–12) were derived from 3 independent experiments and shown as means ± SDs. Statistical significance was determined by a 2-tailed unpaired Student's t test. (F) The overview of polysome profiling assays. KLF16 expression was knocked down by specific siRNA. After 36 h of the transfection, siNC and siKLF16 SW480 cells were exposed to Tg treatment or not. (G) SW480 cells were transfected with indicated siRNAs. After 48 h of transfection, global protein synthesis was quantified by puromycylation assay. (H) SW480 cells transfected with the indicated siRNAs. After 48 h of transfection, cells were treated with or without Tg and followed by WB assays.

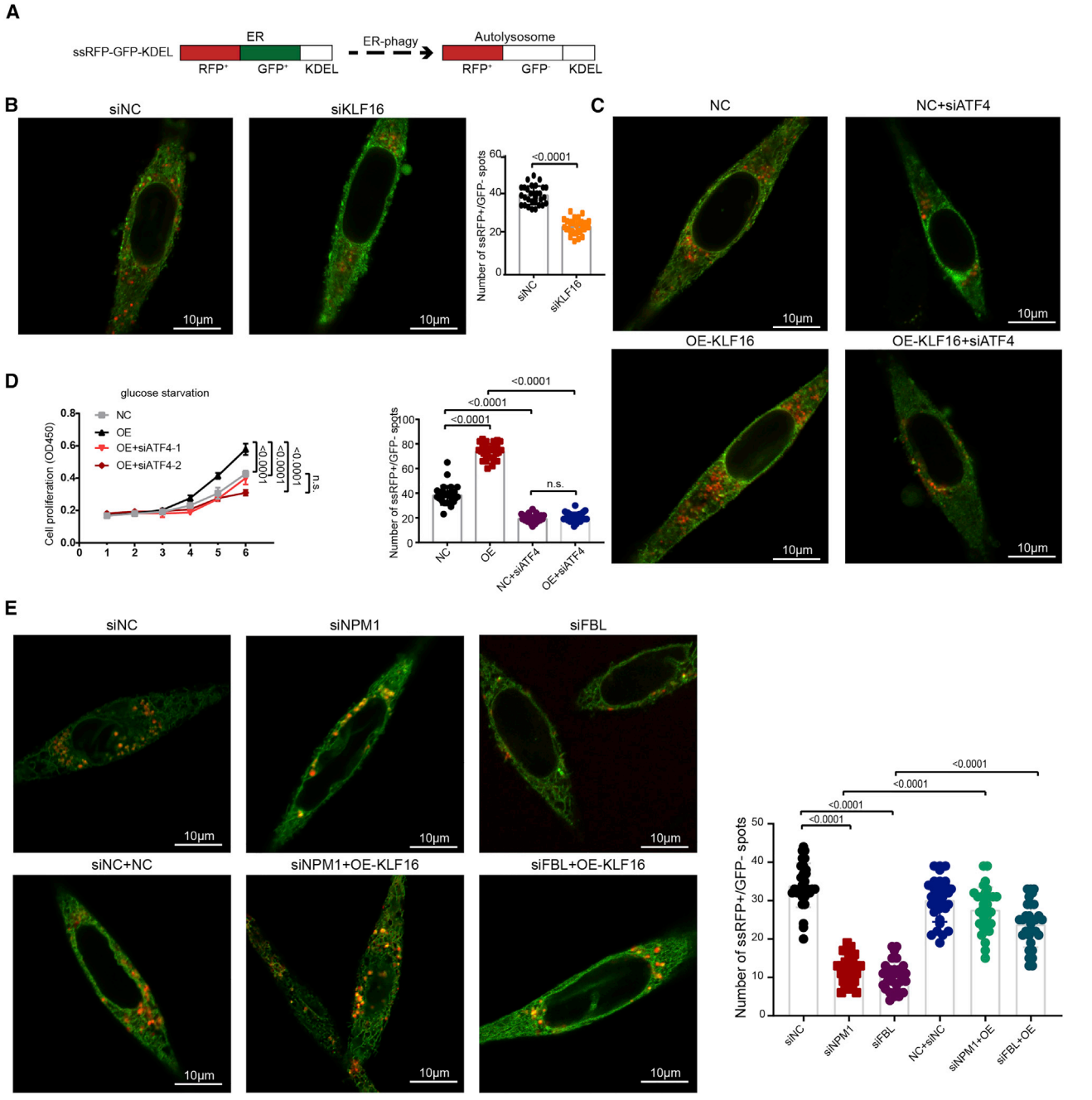

Figure 6. KLF16 upregulates ER-phagy in the UPR

(A) Diagram of ssRFP-GFP-KDEL reporter of ER-phagy. (B) After 12 h of the transfection with ssRFP-GFP-KDEL plasmids, SW480 cells were then transfected with indicated siRNA. After 24 h of the transfection, cells were exposed to glucose starvation conditions for 30 h. Representative images and number of ssRFP^{+}/GFP^{-} spots in siNC and siKLF16 SW480 cells during ER stress. The means ± SDs of the quantification of 30 cells from 3 biologically independent experiments are shown. Statistical significance was determined by a 2-tailed unpaired Student's t test. Scale bar, 10 μm. (C) ssRFP-GFP-KDEL plasmids and OE-KLF16 plasmids were transfected into SW480 cells. After 12 h of the first transfection, cells were then transfected with indicated siRNA. After 24 h of the second transfection, cells were exposed to glucose starvation conditions for 30 h. Representative images and number of ssRFP^{+}/GFP^{-} spots in NC or OE-KLF16 SW480 cells with or without ATF4 knockdown during ER stress. The means ± SDs of the quantification of 30 cells from 3 biologically independent experiments are shown. Statistical significance was determined by a 2-tailed unpaired Student's t test. Scale bar, 10 μm . (D) CCK-8 assays assessed the proliferative capacity of NC or OE-KLF16 SW480 cells with or without ATF4 knockdown. Data represent the means ± SDs from n = 4

(legend continued on next page)

specific molecular mechanisms that regulate the KLF16/NPM1/FBL complex and the nucleolar recruitment of KLF16 during stress.

Abundant endogenous stress-sensitive proteins reversibly enter the nucleolus upon stress and associate with NPM1.[41] NPM1 knockdown decreased the nucleolar localization of KLF16, but our data do not determine that the translocation is directly mediated by NPM1 or simply the result of nucleolar dyshomeostasis. The NTD of NPM1 mediates its oligomerization and interaction with arginine-rich proteins.[30,37] The CTD of NPM1 is required for binding with nucleotides as well as nucleolar localization.[36,71] Each domain of NPM1 is crucial for its roles in nucleolar organization and liquid-liquid phase separation.[37,38] We found that the NPMΔCTD mutant failed to localize to the nucleolus, whereas the other mutants and the FL NPM1 were enriched in the nucleolus. Moreover, NPMΔCTD failed to interact with KLF16 and FBL. Therefore, the CTD of NPM1 is essential for the formation of the KLF16/NPM1/FBL complex.

Recognizing translational regulators that are preferentially overexpressed in cancers can be envisioned to provide potential therapeutic targets.[72] In this study, we revealed that upregulated KLF16 serves as a predictive factor of poor prognosis in CRC patients and may be accompanied by significant cellular stress adaptation. We show that KLF16 interacts with NPM1 and FBL to regulate nucleolar homeostasis and translational reprogramming during ER stress, and thus to enhance stress tolerance and pathogenesis in CRC. Importantly, we also valued the contribution of ATF4-dependent ER-phagy to KLF16-driven CRC carcinogenesis. These findings provide insight into the role of ER stress and nucleolar homeostasis in CRC pathogenesis and identify possible targets for therapy.

MATERIALS AND METHODS

Cell culture

Cell lines were purchased from American Type Culture Collection (ATCC) and maintained in a humidified incubator with 5% CO_2 at 37°C. SW480 and DLD-1 cells were cultured in Roswell Park Memorial Institute 1640 (#C11875500BT Invitrogen, Waltham, MA, USA), and 293T cells were cultured in Dulbecco's modified Eagle's medium (DMEM) (#C11995500BT, Invitrogen). For the glucose starvation assays, cells were cultured in DMEM, not glucose medium (#11966025, Invitrogen). All of the media were supplemented with 10% fetal bovine serum (FBS) (PAN, Adenbach, DER, #ST30-3302) and 1×penicillin-streptomycin solution (#BL505A, Biosharp, Hefei, China).

Patients and samples

All of the tissues were collected from patients who underwent operations between 2006 and 2012 at the Sun Yat-sen University Cancer Center (SYSUCC), Guangzhou, China. A total of 145 cases of II/III CRC tissue samples (including adjacent healthy tissues) and another cohort of 106 cases of stage I/II CRC tissue samples were used. The CRC cases were selected as following inclusion criteria: clear pathological diagnosis, complete follow-up data, and the absence of previous local or systemic treatment. The tumor grade and stage were defined according to the criteria of the World Health Organization (WHO) and the sixth edition of the TNM classification of the International Union Against Cancer. The institutional review board of SYSUCC approved this study.

Animal study

Athymic nude mice were purchased from Vital River Laboratories (Beijing, China), housed under standard conditions in the animal care facility at the Center of Experimental Animal of SYSCC. A total of 3×10^6 DLD-1 cells with lentivirus-mediated stable knockdown or stable overexpression of KLF16 were injected subcutaneously into the dorsal flanks of 4- and 5-week-old female athymic nude mice (n = 6/group). After 2 weeks, mice were sacrificed, and tumors were excised and weighed.

All of the procedures were approved by the Sun Yat-sen University Animal Care and Use Committee.

siRNA and plasmid transfection

The siRNAs specifically targeting KLF16, NPM1, FBL, and ATF4, and normal control siRNA (siNC) were synthesized by RiboBio (Guangzhou, CHN). The siRNAs were transfected with LIPOFECTAMINE 2000 (#11668019, Invitrogen) or with INTERFERin (#409-10, Polyplus Transfection, Strasbourg, France).

The short hairpin RNAs (shRNAs) of KLF16, rDNA promoter-reporter, and translation-reporter plasmids were modified by FulenGene (Guangzhou, China). For the construction of the translation reporter, we modified a pGL3-Rluc-X-luciferase plasmid, which can transcribe a single mRNA both encode renilla luciferase and firefly luciferase, and the translational regulatory sequence of target genes are inserted in between. The sequence of IRESs was obtained from IRESbase (http://reprod.njmu.edu.cn/cgi-bin/iresbase/index.php).

KLF16 and NPM1 FL or truncated mutant plasmids were purchased from GeneCreate Biotech (Wuhan, China). The ER-phagy reporter pCW57-CMV-ssRFP-GFP-KDEL was obtained from Addgene (128257; Watertown, MA, USA). LIPOFECTAMINE 2000 or jetPRIME (#114-15, Polyplus Transfection) were used for plasmids transfection.

Western blotting (WB) and IP assay

Cells were harvested and lysed by IP lysis buffer (25 mM Tris-HCl, 150 M NaCl, 1 mM EDTA, 1% NP40, 5% glycerin) supplemented

biologically independent experiments. Statistical significance was determined by a 2-way ANOVA. (E).ssRFP-GFP-KDEL plasmids and indicated plasmids were transfected into SW480 cells. After 12 h of the first transfection, cells were then transfected with indicated siRNA. After 24 h of the second transfection, cells were exposed to glucose starvation condition for 30h. Representative images and number of ssRFP+/GFP- spots in SW480 cells. The mean ± SD of the quantification of 30 cells from 3 biologically independent experiments is shown. Statistical significance was determined by a two-tailed unpaired Student's t test. Scale bar, 10 μm.

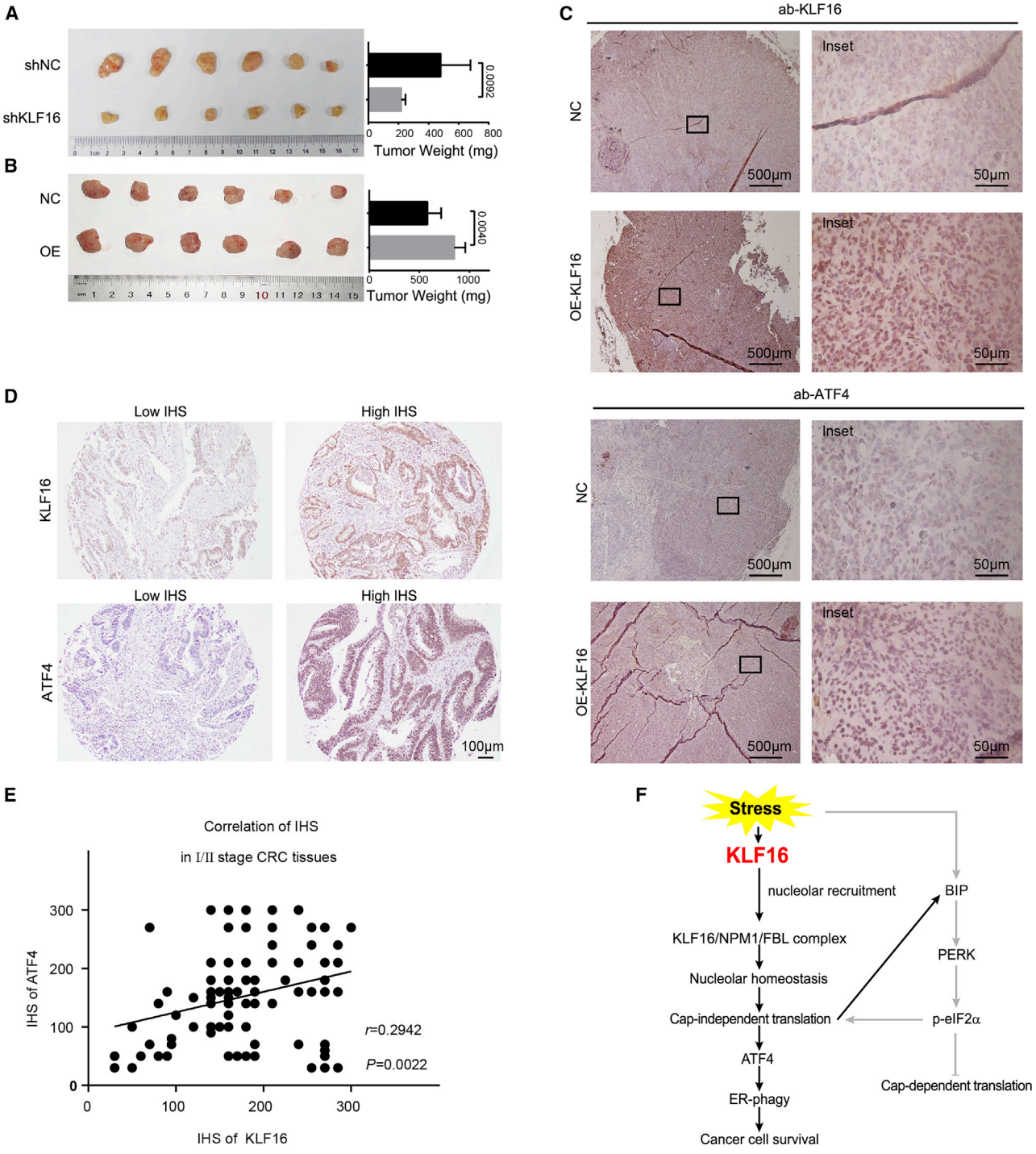

Figure 7. ATF4 is correlated with KLF16 in xenograft and CRC tissue samples

(A) 3×10^6 DLD-1 cells with lentivirus-mediated stable knockdown of KLF16 were implanted into nude mice (n = 6) for xenograft tumor models. Images and weights of the tumors are presented. Data represent the means ± SDs of the tumor weight. Statistical significance was determined by a 2-tailed unpaired Student's t test. (B) 3×10^6 DLD-1 cells with lentivirus-mediated stable OE of KLF16 were implanted into nude mice (n = 6) for xenograft tumor models. Images and weights of the tumors are presented. Data represent the means ± SDs of the tumor weight. Statistical significance was determined by a 2-tailed unpaired Student's t test. (C) Representative IHC staining for KLF16 and ATF4 in CRC xenograft tumor tissues samples. Scale bar, 100 μm. (D) Representative IHC staining images of low immunohistochemical score (IHS) and high IHS in stage I/II CRC tissues with the indicated antibodies. Scale bar, 100 μm. (E) The correlation of IHS was evaluated using Pearson's correlation analysis. (F) Schematic depicting functions of KLF16 during ER stress.

with protease inhibitor cocktail. Equal amounts of protein lysates were resolved by 10% SDS-PAGE gels and then transferred on a polyvinylidene fluoride (PVDF) membrane (#3010040001, Roche, Basel, Switzerland). After blocking using 5% milk, the membrane was incubated with the primary antibody at 4°C overnight, then hybridized with a secondary antibody at room temperature (RT) for 1 h. The immunoreactive signals were visualized by High-sig ECL Western Blotting Peroxide Buffer (#180-5001W, Tanon, Shanghai, China).

For IP experiments, cell extracts were pre-cleared by incubation with Dynabeads protein A/G (#10002D/10004D, Invitrogen) for 1 h at 4°C in a roll shaker. Thereafter, antibodies were mixed into the lysates with newly added Dynabeads and incubated at 4°C overnight. Immunocomplexes were collected on a magnetic separator, washed five times with IP lysis buffer, and eluted in 1× SDS sample buffer for WB analysis. The antibodies used in this study are listed in Table S3.

Silver staining and LC-MS/MS analysis

Silver staining was performed using the Fast Silver Stain Kit (#P0017S, Beyotime, Shanghai, China) as the protocol described, while LC-MS/MS and protein identification and quantification were accomplished by BGI (Shenzhen, China). Gel electrophoresis is used to separate the sample proteins, and then the peptides were extracted from protein gel strips after enzymatic digestion. LC-MS/MS (UltiMate 3000 UHPLC [ultra-high performance liquid chromatography] and Q-Exactive HF X, Thermo Fisher Scientific, Waltham, MA, USA) is used to obtain the mass spectrum of the proteins in these gel strips, and finally the protein identification software is used to identify the proteins in the samples.

Puromycylation assay

To analysis global protein synthesis, cells were pretreated with the elongation inhibitor cycloheximide (CHX) (100 μg/mL) for 10 min. Then, 10 μg/mL puromycin was incorporated in the culture medium for 30 min at 37°C. The whole-cell protein extracts were immediately prepared, and the nascent polypeptide chain was detected by WB assay using a specific anti-puromycin antibody.

RNA extraction and quantitative real-time PCR analysis

Total RNA extraction was performed using the TRIzol reagent (#15596018, Invitrogen) following the manufacturer's instructions. The obtained RNA was then reverse transcribed into complementary DNA using a Prime Script RT Reagent Kit (#RR036A Takara Bio, Dalian, China) and diluted 1:10 in double-distilled water to use as a template for quantitative real-time PCR, which was carried out with iTaq Univer SYBR Green Supermix (#1725122Bio-Rad Laboratories, Hercules, CA, USA). The primer sequences are listed in Table S4.

Isolation of cytoplasmic and nuclear RNA

Cytoplasmic and nuclear RNA fractions were isolated by using the reagents supplied in the PARIS Kit (#AM1556, Thermo Fisher Scientific). Briefly, cells were lysed in cell fraction buffer on ice for 10 min. After centrifugation at 500 × *g* for 3 min at 4°C, the supernatant was collected as the cytoplasmic fraction. For nucleolus isolation, the pellet was dissolved in cell disruption buffer. Then, the RNA isolation followed the manufacturer's instructions.

Polysomal fractionation

For polysome preparation, cells were incubated with CHX (100 μg/mL) for 10 min and then washed with ice-cold PBS containing CHX (100 μg/mL). Thereafter, cells were scraped and collected in polysome extraction buffer (10 mM Tris-HCl, 5 mM $MgCl_2$, and 100 mM KCl, 100 μg/mL CHX, 2 mM DTT [#707265ML, Invitrogen], 20 U/mL RNase inhibitor (#N8080119, Invitrogen], EDTA-free protease inhibitors [#4693132001-1, Roche], 1% Triton X-100). The nuclei and debris were discarded after a 16,000 × *g*, 10-min centrifugation. Then, 500 μL supernatant fluid was loaded on a 10%–50% sucrose gradient (20 mM HEPES-KOH, 5 mM $MgCl_2$, 100 mM KCl, 100 μg/mL CHX, 2 mM DTT, and 10 U/mL RNase inhibitor) and centrifuged for 2 h at 36,000 rpm at 4°C in a Beckman SW41Ti rotor. Polysome profiles were reordered using a UA-6 absorbance detector connected to the fraction collector and measuring absorbance at 260 nm. RNA from each fraction was subsequently extracted with TRIzol. The cDNA was separated by 2% agarose gel electrophoresis and visualized by ethidium bromide staining or subjected to quantitative real-time PCR assay for further analysis.

Cell Counting Kit-8 (CCK-8) assay

We used the CCK-8 (HY-K0301, MCE, Monmouth Junction, NJ, USA) to measure the proliferation of DLD-1 and SW480 cells. A total of 1200 cells were cultured in 4 replicate wells in a 96-well plate. Then, 10 μL CCK-8 reagent was added to 90 μL FBS free medium to generate a working solution, 100 μL of which was added per well and incubated for 2 h. Finally the absorbance was measured at 450 nm.

EU labeling assay

To capture the newly synthesized nascent RNAs, 0.2 mM EU was added to the culture medium for 2 h at 37°C. EU-incorporated RNAs were visualized by using the Cell-Light EU Apollo 488 In Vitro Imaging Kit (#C10316-3, RiboBio) in accordance with the manufacturer's instructions.

IF staining

The cells were fixed with 4% formaldehyde solution for 20 min and then washed with PBS solution 3 times at RT. Subsequently, the cells were permeabilized with 0.5% Triton X-100 in PBS solution for 30 min. After blocking with 5% BSA in PBS at RT for 1 h, the cells were incubated with primary antibody diluted in blocking solution at 4°C overnight. The following day, the cells were incubated with the secondary antibodies for Alexa Fluor 488 (#SA00003, Proteintech, Rosemont, IL, USA) and Alexa Fluor 594 at RT for 1 h. Then, the cells were stained with DAPI for 10 min and washed 3 times for 5 min with PBS. Epifluorescence images were imaged with a Zeiss LSM880 microscope (Zeiss, White Plains, NY, USA).

For the RNase R treatment, the living cells were pre-permeabilized with 0.05% Triton X-100, and then 1 mg/mL RNase A was used for 10 min at RT before staining.

Reporter luciferase assay

For luciferase reporter assays, cells were transfected with translation-reporter plasmids or rDNA promoter-reporter. Thirty-six hours after transfection, luciferase activity was measured using the Dual Luciferase Reporter Assay Kit (#DL101-01, Vazyme Biotech, Nangjing, China) following the manufacturer's instructions.

IHC staining

Paraffin-embedded sections were deparaffinized and rehydrated and were then subjected to antigen retrieval for 8 min in EDTA (pH = 8.0). After the sections were cooled to RT, 3% H_2O_2 was used to block endogenous peroxidases. The sections were blocked with 10% BSA and incubated with the anti-KLF16 or anti-ATF4 primary antibody at a 1:100 dilution overnight at 4°C. After incubation with the secondary antibody, immunodetection was performed with DAB staining (#DAB-0031MXB, Fuzhou, China,). The immunohistochemical score (IHS) of KLF16 and ATF4 were determined by combining the staining intensity score (1, negative; 2, weak staining; 3, moderate staining; 4, strong staining) and the percentage of positively stained tumor cells.

Statistical analysis

All of the experiments were carried out at least 3 times and presented as mean ± standard deviation (SD). We have indicated the n values used for each analysis in the figure captions. Statistical analyses were performed using GraphPad Prism (version 7.0; GraphPad, San Diego, CA, USA) or SPSS (version 19.0, SPSS Statistics, Armonk, NY, USA).

For survival analysis, the median was used as the optimal cutpoint for KLF16 expression. The correlation between KLF16 and the clinicopathological features of patients with CRC was analyzed using the χ^2 test or Fisher's exact test. For univariate survival analysis, survival curves were obtained using the Kaplan-Meier method. The Cox proportional hazards regression model was used for multivariate survival analyses. Pearson's correlation was used to analyze the relative IHS of KLF16 and ATF4. Other measurements were analyzed using a two-tailed Student's *t* test or analysis of variance (ANOVA) where appropriate.

Ethical Approval and Consent to participate

The use of human CRC tissue specimens in this study was approved by the ethics committee of the Sun Yat-sen University Cancer Center. All animal studies were approved by the IACUC of Sun Yat-sen University and performed according with ethical requirement for animal experiments.

Data availability

The data generated in this study are available within the article and the supplemental information.

SUPPLEMENTAL INFORMATION

Supplemental information can be found online at https://doi.org/10.1016/j.ymthe.2022.04.022.

ACKNOWLEDGMENTS

This work was supported by grants from the National Natural Science Foundation of China (grant nos. 81972227, 81730072, 82072608, 81872001, and 82002467); the Natural Science Foundation of Guangdong (grant numbers 2020A151501021 and 2020A1515011020); the Guangzhou Science and Technology Plan Projects (grant no. 201904020044), and the China Postdoctoral Science Foundation (2020M672999).

AUTHOR CONTRIBUTIONS

F.-W.W. and D.X. conceived and devised the study. X.-D.M. and F.-W.W. designed the experiments and analysis. X.-D.M., S.-D.X., S.-H.H., H.L., R.-X.C., X.-H. J., J.-H.C., and J.-L.L. performed the experiments. K.H. and J.-W.C. performed the bioinformatics and statistical analyses. X.-D.M., S.-D.X., and S.-H.H analyzed and interpreted the data. Q.-J.O., Y.-J.F., and Z.-Z.P. provided CRC patient tissue samples and clinical information. D.X. and F.-W.W. supervised the research, and together with X.-D.M., S.-D.X., and S.-H.H. wrote the manuscript. All of the authors approved the submitted manuscript.

DECLARATION OF INTERESTS

The authors declare no competing interests.

REFERENCES

1. Chen, X., and Cubillos-Ruiz, J.R. (2021). Endoplasmic reticulum stress signals in the tumour and its microenvironment. Nat. Rev. Cancer *21*, 71–88. https://doi.org/10.1038/s41568-020-00312-2.

2. Cubillos-Ruiz, J.R., Bettigole, S.E., and Glimcher, L.H. (2017). Tumorigenic and immunosuppressive effects of endoplasmic reticulum stress in cancer. Cell *168*, 692–706. https://doi.org/10.1016/j.cell.2016.12.004.

3. Hamanaka, R., Bennett, B.S., Bennett, B., Cullinan, S.B., Cullinan, S., Diehl, J.A., and Diehl, J. (2005). PERK and GCN2 contribute to eIF2α phosphorylation and cell cycle arrest after activation of the unfolded protein response pathway. Mol. Biol. Cell *16*, 5493–5501. https://doi.org/10.1091/mbc.e05-03-0268.

4. Jackson, R.J., Hellen, C.U.T., and Pestova, T.V. (2010). The mechanism of eukaryotic translation initiation and principles of its regulation. Nat. Rev. Mol. Cell Biol. *11*, 113–127. https://doi.org/10.1038/nrm2838.

5. Jaud, M., Philippe, C., Di Bella, D., Tang, W., Pyronnet, S., Laurell, H., Mazzolini, L., Rouault-Pierre, K., and Touriol, C. (2020). Translational regulations in response to endoplasmic reticulum stress in cancers. Cells *9*, 540. https://doi.org/10.3390/cells9030540.

6. Zielke, S., Kardo, S., Zein, L., Mari, M., Covarrubias-Pinto, A., Kinzler, M.N., Meyer, N., Stolz, A., Fulda, S., Reggiori, F., et al. (2020). ATF4 links ER stress with reticulophagy in glioblastoma cells. Autophagy *17*, 2432–2448. https://doi.org/10.1080/15548627.2020.1827780.

7. Hetz, C., Zhang, K., and Kaufman, R.J. (2020). Mechanisms, regulation and functions of the unfolded protein response. Nat. Rev. Mol. Cell Biol. *21*, 421–438. https://doi.org/10.1038/s41580-020-0250-z.

8. You, K., Wang, L., Chou, C.H., Liu, K., Nakata, T., Jaiswal, A., Yao, J., Lefkovith, A., Omar, A., Perrigoue, J.G., et al. (2021). QRICH1 dictates the outcome of ER stress through transcriptional control of proteostasis. Science *371*. https://doi.org/10.1126/science.abb6896.

9. Pecoraro, A., Pagano, M., Russo, G., and Russo, A. (2020). Role of autophagy in cancer cell response to nucleolar and endoplasmic reticulum stress. Int. J. Mol. Sci. *21*, 7334. https://doi.org/10.3390/ijms21197334.

10. Sung, H., Ferlay, J., Siegel, R., Laversanne, M., Soerjomataram, I., Jemal, A., and Bray, F. (2021). Global cancer statistics 2020: GLOBOCAN estimates of incidence and mortality worldwide for 36 cancers in 185 countries. CA Cancer J. Clin. *71*, 209–249. https://doi.org/10.3322/caac.21660.

11. Huang, J., Pan, H., Wang, J., Wang, T., Huo, X., Ma, Y., Lu, Z., Sun, B., and Jiang, H. (2021). Unfolded protein response in colorectal cancer. Cell Biosci. *11*, 26. https://doi.org/10.1186/s13578-021-00538-z.

12. Zhang, Y.h., Cui, S.x., Wan, S.b., Wu, S.h., and Qu, X.j. (2021). Increased S1P induces S1PR2 internalization to blunt the sensitivity of colorectal cancer to 5-fluorouracil via promoting intracellular uracil generation. Acta Pharmacol. Sinica *42*, 460–469. https://doi.org/10.1038/s41401-020-0460-0.

13. Coleman, O.I., Lobner, E.M., Bierwirth, S., Sorbie, A., Waldschmitt, N., Rath, E., Berger, E., Lagkouvardos, I., Clavel, T., McCoy, K.D., et al. (2018). Activated ATF6 induces intestinal dysbiosis and innate immune response to promote colorectal tumorigenesis. Gastroenterology *155*, 1539–1552.e12. https://doi.org/10.1053/j.gastro.2018.07.028.

14. Tang, C.H.A., Ranatunga, S., Kriss, C.L., Cubitt, C.L., Tao, J., Pinilla-Ibarz, J.A., Del Valle, J.R., and Hu, C.C.A. (2014). Inhibition of ER stress-associated IRE-1/XBP-1 pathway reduces leukemic cell survival. J. Clin. Invest. *124*, 2585–2598. https://doi.org/10.1172/jci73448.

15. Zhao, N., Cao, J., Xu, L., Tang, Q., Dobrolecki, L.E., Lv, X., Talukdar, M., Lu, Y., Wang, X., Hu, D.Z., et al. (2018). Pharmacological targeting of MYC-regulated IRE1/XBP1 pathway suppresses MYC-driven breast cancer. J. Clin. Invest. *128*, 1283–1299. https://doi.org/10.1172/jci95873.

16. Atkins, C., Liu, Q., Minthorn, E., Zhang, S.Y., Figueroa, D.J., Moss, K., Stanley, T.B., Sanders, B., Goetz, A., Gaul, N., et al. (2013). Characterization of a novel PERK kinase inhibitor with antitumor and antiangiogenic activity. Cancer Res. *73*, 1993–2002. https://doi.org/10.1158/0008-5472.can-12-3109.

17. Kim, C.K., He, P., Bialkowska, A.B., and Yang, V.W. (2017). SP and KLF transcription factors in digestive physiology and diseases. Gastroenterology *152*, 1845–1875. https://doi.org/10.1053/j.gastro.2017.03.035.

18. Takahashi, K., and Yamanaka, S. (2016). A decade of transcription factor-mediated reprogramming to pluripotency. Nat. Rev. Mol. Cell Biol. *17*, 183–193. https://doi.org/10.1038/nrm.2016.8.

19. Yang, V.W., Liu, Y., Kim, J., Shroyer, K.R., and Bialkowska, A.B. (2019). Increased genetic instability and accelerated progression of colitis-associated colorectal cancer through intestinal epithelium–specific deletion of *Klf4*. Mol. Cancer Res. *17*, 165–176. https://doi.org/10.1158/1541-7786.mcr-18-0399.

20. Morimoto, Y., Mizushima, T., Wu, X., Okuzaki, D., Yokoyama, Y., Inoue, A., Hata, T., Hirose, H., Qian, Y., Wang, J., et al. (2020). miR-4711-5p regulates cancer stemness and cell cycle progression via KLF5, MDM2 and TFDP1 in colon cancer cells. Br. J. Cancer *122*, 1037–1049. https://doi.org/10.1038/s41416-020-0758-1.

21. Takagi, Y., Sakai, N., Yoshitomi, H., Furukawa, K., Takayashiki, T., Kuboki, S., Takano, S., Suzuki, D., Kagawa, S., Mishima, T., et al. (2020). High expression of Krüppel-like factor 5 is associated with poor prognosis in patients with colorectal cancer. Cancer Sci. *111*, 2078–2092. https://doi.org/10.1111/cas.14411.

22. Sun, N., Shen, C., Zhang, L., Wu, X., Yu, Y., Yang, X., Yang, C., Zhong, C., Gao, Z., Miao, W., et al. (2020). Hepatic Krüppel-like factor 16 (KLF16) targets PPARα to improve steatohepatitis and insulin resistance. Gut *70*, 2183–2195. https://doi.org/10.1136/gutjnl-2020-321774.

23. Zhang, J., Yu, W., Wang, X., Hu, B., Wu, D., and Shi, G. (2020). KLF16 affects the MYC signature and tumor growth in prostate cancer. OncoTargets Ther. *13*, 1303–1310. https://doi.org/10.2147/ott.s233495.

24. Daftary, G.S., Lomberk, G.A., Buttar, N.S., Allen, T.W., Grzenda, A., Zhang, J., Zheng, Y., Mathison, A.J., Gada, R.P., Calvo, E., et al. (2012). Detailed structural-functional analysis of the Krüppel-like factor 16 (KLF16) transcription factor reveals novel mechanisms for silencing Sp/KLF sites involved in metabolism and endocrinology. J. Biol. Chem. *287*, 7010–7025. https://doi.org/10.1074/jbc.M111.266007.

25. Chen, Z., Huang, Q., Xu, W., Wang, H., Yang, J., and Zhang, L.J. (2020). PRKD3 promotes malignant progression of OSCC by downregulating KLF16 expression. Eur. Rev. Med. Pharmacol. Sci. *24*, 12709–12716. https://doi.org/10.26355/eurrev_202012_24169.

26. Prestes, E., Bruno, J.C.P., Bruno, J., Travassos, L.H., Travassos, L., Carneiro, L.A.M., and Carneiro, L. (2021). The unfolded protein response and autophagy on the crossroads of coronaviruses infections. Front. Cell. Infect. Microbiol. *11*, 668034. https://doi.org/10.3389/fcimb.2021.668034.

27. Tafforeau, L., Zorbas, C., Langhendries, J.L., Mullineux, S.T., Stamatopoulou, V., Mullier, R., Wacheul, L., and Lafontaine, D. (2013). The complexity of human ribosome biogenesis revealed by systematic nucleolar screening of Pre-rRNA processing factors. Mol. Cell *51*, 539–551. https://doi.org/10.1016/j.molcel.2013.08.011.

28. Gueiderikh, A., Maczkowiak-Chartois, F., Rouvet, G., Souquère-Besse, S., Apcher, S., Diaz, J.J., and Rosselli, F. (2021). Fanconi anemia A protein participates in nucleolar homeostasis maintenance and ribosome biogenesis. Sci. Adv. *7*, eabb5414. https://doi.org/10.1126/sciadv.abb5414.

29. Espinoza, J.A., Zisi, A., Kanellis, D., Carreras-Puigvert, J., Henriksson, M., Hühn, D., Watanabe, K., Helleday, T., Lindstrom, M.S., and Bartek, J. (2020). The antimalarial drug amodiaquine stabilizes p53 through ribosome biogenesis stress, independently of its autophagy-inhibitory activity. Cell Death Differ. *27*, 773–789. https://doi.org/10.1038/s41418-019-0387-5.

30. Mitrea, D.M., Grace, C.R., Buljan, M., Yun, M.K., Pytel, N.J., Satumba, J., Nourse, A., Park, C.G., Madan Babu, M., White, S.W., and Kriwacki, R.W. (2014). Structural polymorphism in the N-terminal oligomerization domain of NPM1. Proc. Natl. Acad. Sci. U S A *111*, 4466–4471. https://doi.org/10.1073/pnas.1321007111.

31. Vascotto, C., Fantini, D., Romanello, M., Cesaratto, L., Deganuto, M., Leonardi, A., Radicella, J.P., Kelley, M.R., D'Ambrosio, C., Scaloni, A., et al. (2009). APE1/Ref-1 interacts with NPM1 within nucleoli and plays a role in the rRNA quality control process. Mol. Cell Biol. *29*, 1834–1854. https://doi.org/10.1128/mcb.01337-08.

32. Huang, N., Negi, S., Szebeni, A., and Olson, M.O. (2005). Protein NPM3 interacts with the multifunctional nucleolar protein B23/nucleophosmin and inhibits ribosome biogenesis. J. Biol. Chem. *280*, 5496–5502. https://doi.org/10.1074/jbc.M407856200.

33. Chen, Z., Lei, T., Chen, X., Zhang, J., Yu, A., Long, Q., Long, H., Jin, D., Gan, L., and Yang, Z. (2010). Porcine KLF gene family: structure, mapping, and phylogenetic analysis. Genomics *95*, 111–119. https://doi.org/10.1016/j.ygeno.2009.11.001.

34. Rodríguez, E., Aburjania, N., Priedigkeit, N.M., DiFeo, A., and Martignetti, J.A. (2010). Nucleo-cytoplasmic localization domains regulate Krüppel-like factor 6 (KLF6) protein stability and tumor suppressor function. PLoS One *5*, e12639. https://doi.org/10.1371/journal.pone.0012639.

35. Shields, J.M., and Yang, V.W. (1997). Two potent nuclear localization signals in the gut-enriched Krüppel-like factor define a subfamily of closely related Krüppel proteins. J. Biol. Chem. *272*, 18504–18507. https://doi.org/10.1074/jbc.272.29.18504.

36. Wang, X., Hu, X., Song, W., Xu, H., Xiao, Z., Huang, R., Bai, Q., Zhang, F., Chen, Y., Liu, Y., et al. (2021). Mutual dependency between lncRNA LETN and protein NPM1 in controlling the nucleolar structure and functions sustaining cell proliferation. Cell Res. *31*, 664–683. https://doi.org/10.1038/s41422-020-00458-6.

37. Mitrea, D.M., Cika, J.A., Guy, C.S., Ban, D., Banerjee, P.R., Stanley, C.B., Nourse, A., Deniz, A.A., and Kriwacki, R.W. (2016). Nucleophosmin integrates within the nucleolus via multi-modal interactions with proteins displaying R-rich linear motifs and rRNA. Elife *5*, e13571. https://doi.org/10.7554/eLife.13571.

38. Mitrea, D.M., Cika, J.A., Stanley, C.B., Nourse, A., Onuchic, P.L., Banerjee, P.R., Phillips, A.H., Park, C.G., Deniz, A.A., and Kriwacki, R.W. (2018). Self-interaction of NPM1 modulates multiple mechanisms of liquid-liquid phase separation. Nat. Commun. *9*, 842. https://doi.org/10.1038/s41467-018-03255-3.

39. Lopez, D.J., Rodriguez, J.A., and Banuelos, S. (2020). Nucleophosmin, a multifunctional nucleolar organizer with a role in DNA repair. Biochim. Biophys. Acta Proteins Proteomics *1868*, 140532. https://doi.org/10.1016/j.bbapap.2020.140532.

40. Weeks, S.E., Metge, B.J., and Samant, R.S. (2019). The nucleolus: a central response hub for the stressors that drive cancer progression. Cell Mol. Life Sci. *76*, 4511–4524. https://doi.org/10.1007/s00018-019-03231-0.

41. Frottin, F., Schueder, F., Tiwary, S., Gupta, R., Körner, R., Schlichthaerle, T., Cox, J., Jungmann, R., Hartl, F.U., and Hipp, M.S. (2019). The nucleolus functions as a phase-separated protein quality control compartment. Science *365*, 342–347. https://doi.org/10.1126/science.aaw9157.

42. Boisvert, F.M., van Koningsbruggen, S., Navascués, J., and Lamond, A.I. (2007). The multifunctional nucleolus. Nat. Rev. Mol. Cell Biol. *8*, 574–585. https://doi.org/10.1038/nrm2184.

43. Ghoshal, K., Majumder, S., Datta, J., Motiwala, T., Bai, S., Sharma, S.M., Frankel, W., and Jacob, S.T. (2004). Role of human ribosomal RNA (rRNA) promoter methylation and of methyl-CpG-binding protein MBD2 in the suppression of rRNA gene expression. J. Biol. Chem. *279*, 6783–6793. https://doi.org/10.1074/jbc.M309393200.

44. Teschler, S., Gotthardt, J., Dammann, G., and Dammann, R. (2016). Aberrant DNA methylation of rDNA and PRIMA1 in borderline personality disorder. Int. J. Mol. Sci. *17*, 67. https://doi.org/10.3390/ijms17010067.

45. Buchwalter, A., and Hetzer, M.W. (2017). Nucleolar expansion and elevated protein translation in premature aging. Nat. Commun. *8*, 328. https://doi.org/10.1038/s41467-017-00322-z.

46. Mende, H., and Müller, S. (2021). Surveillance of nucleolar homeostasis and ribosome maturation by autophagy and the ubiquitin-proteasome system. Matrix Biol. *100-101*, 30–38. https://doi.org/10.1016/j.matbio.2021.02.001.

47. Sun, Z., Yu, H., Zhao, J., Tan, T., Pan, H., Zhu, Y., Chen, L., Zhang, C., Zhang, L., Lei, A., et al. (2021). LIN28 coordinately promotes nucleolar/ribosomal functions and represses the 2C-like transcriptional program in pluripotent stem cells. Protein Cell. https://doi.org/10.1007/s13238-021-00864-5.

48. Krogh, N., Jansson, M.D., Häfner, S.J., Tehler, D., Birkedal, U., Christensen-Dalsgaard, M., Lund, A.H., and Nielsen, H. (2016). Profiling of 2'-O-Me in human rRNA reveals a subset of fractionally modified positions and provides evidence for ribosome heterogeneity. Nucleic Acids Res. *44*, 7884–7895. https://doi.org/10.1093/nar/gkw482.

49. Erales, J., Marchand, V., Panthu, B., Gillot, S., Belin, S., Ghayad, S., Garcia, M., Laforets, F., Marcel, V., Baudin-Baillieu, A., et al. (2017). Evidence for rRNA 2'-O-methylation plasticity: control of intrinsic translational capabilities of human ribosomes. Proc. Natl. Acad. Sci. U S A *114*, 12934–12939. https://doi.org/10.1073/pnas.1707674114.

50. Nachmani, D., Bothmer, A.H., Grisendi, S., Mele, A., Bothmer, D., Lee, J.D., Monteleone, E., Cheng, K., Zhang, Y., Bester, A.C., et al. (2019). Germline NPM1 mutations lead to altered rRNA 2'-O-methylation and cause dyskeratosis congenita. Nat. Genet. *51*, 1518–1529. https://doi.org/10.1038/s41588-019-0502-z.

51. Yi, Y., Li, Y., Meng, Q., Li, Q., Li, F., Lu, B., Shen, J., Fazli, L., Zhao, D., Li, C., et al. (2021). A PRC2-independent function for EZH2 in regulating rRNA 2'-O methylation and IRES-dependent translation. Nat. Cell Biol. *23*, 341–354. https://doi.org/10.1038/s41556-021-00653-6.

52. Vattem, K.M., and Wek, R.C. (2004). Reinitiation involving upstream ORFs regulates ATF4 mRNA translation in mammalian cells. Proc. Natl. Acad. Sci. U S A *101*, 11269–11274. https://doi.org/10.1073/pnas.0400541101.

53. Johannes, G., and Sarnow, P. (1998). Cap-independent polysomal association of natural mRNAs encoding c-myc, BiP, and eIF4G conferred by internal ribosome entry sites. RNA *4*, 1500–1513. https://doi.org/10.1017/s1355838298981080.

54. Smith, M.D., Harley, M.E., Kemp, A.J., Wills, J., Lee, M., Arends, M., von Kriegsheim, A., Behrends, C., and Wilkinson, S. (2018). CCPG1 is a non-canonical autophagy cargo receptor essential for ER-phagy and pancreatic ER proteostasis. Dev. Cell *44*, 217–232.e11. https://doi.org/10.1016/j.devcel.2017.11.024.

55. Chino, H., and Mizushima, N. (2020). ER-phagy: quality control and turnover of endoplasmic reticulum. Trends Cell Biol. *30*, 384–398. https://doi.org/10.1016/j.tcb.2020.02.001.

56. Molinari, M. (2021). ER-phagy responses in yeast, plants, and mammalian cells and their crosstalk with UPR and ERAD. Dev. Cell *56*, 949–966. https://doi.org/10.1016/j.devcel.2021.03.005.

57. Wilkinson, S. (2019). ER-phagy: shaping up and destressing the endoplasmic reticulum. FEBS J. *286*, 14932–22663. https://doi.org/10.1111/febs.14932.

58. Chino, H., Hatta, T., Natsume, T., and Mizushima, N. (2019). Intrinsically disordered protein TEX264 mediates ER-phagy. Mol. Cell *74*, 909–921.e6. https://doi.org/10.1016/j.molcel.2019.03.033.

59. Wang, T., Li, L., Chen, Y., Fu, S., Wu, Z., Du, B., Yang, X., Zhang, W., Hao, X., and Guo, T. (2021). Ribosome assembly factor URB1 contributes to colorectal cancer proliferation through transcriptional activation of ATF4. Cancer Sci. *112*, 101–116. https://doi.org/10.1111/cas.14643.

60. Shi, Z., Yu, X., Yuan, M., Lv, W., Feng, T., Bai, R., and Zhong, H. (2019). Activation of the PERK-ATF4 pathway promotes chemo-resistance in colon cancer cells. Sci. Rep. *9*, 3210. https://doi.org/10.1038/s41598-019-39547-x.

61. Minnee, E., and Faller, W.J. (2021). Translation initiation and its relevance in colorectal cancer. FEBS J. *288*, 6635–6651. https://doi.org/10.1111/febs.15690.

62. Sriram, A., Bohlen, J., and Teleman, A.A. (2018). Translation acrobatics: how cancer cells exploit alternate modes of translational initiation. EMBO Rep. *19*, e45947. https://doi.org/10.15252/embr.201845947.

63. Zhang, B., Wang, J., Wang, X., Zhu, J., Shi, Z., Chambers, M.C., Chambers, M.C., Zimmerman, L.J., Shaddox, K.F., Kim, S., et al. (2014). Proteogenomic characterization of human colon and rectal cancer. Nature *513*, 382–387. https://doi.org/10.1038/nature13438.

64. Pecoraro, A., Pagano, M., Russo, G., and Russo, A. (2021). Ribosome biogenesis and cancer: overview on ribosomal proteins. Int. J. Mol. Sci. *22*, 5496. https://doi.org/10.3390/ijms22115496.

65. DuRose, J.B., Scheuner, D., Kaufman, R.J., Rothblum, L.I., and Niwa, M. (2009). Phosphorylation of eukaryotic translation initiation factor 2α coordinates rRNA transcription and translation inhibition during endoplasmic reticulum stress. Mol. Cell. Biol. *29*, 4295–4307. https://doi.org/10.1128/mcb.00260-09.

66. Harding, H.P., Zhang, Y., Bertolotti, A., Zeng, H., and Ron, D. (2000). Perk is essential for translational regulation and cell survival during the unfolded protein response. Mol. Cell *5*, 897–904. https://doi.org/10.1016/s1097-2765(00)80330-5.

67. Solanki, N.R., Stadanlick, J.E., Zhang, Y., Duc, A.C., Lee, S.Y., Lauritsen, J.P.H., Zhang, Z., and Wiest, D.L. (2016). Rpl22 loss selectively impairs αβ T cell development by dysregulating endoplasmic reticulum stress signaling. J. Immunol. *197*, 2280–2289. https://doi.org/10.4049/jimmunol.1600815.

68. Russo, A., Pagliara, V., Albano, F., Esposito, D., Sagar, V., Loreni, F., Irace, C., Santamaria, R., and Russo, G. (2016). Regulatory role of rpL3 in cell response to nucleolar stress induced by Act D in tumor cells lacking functional p53. Cell Cycle *15*, 41–51. https://doi.org/10.1080/15384101.2015.1120926.

69. Matsuki, Y., Matsuo, Y., Nakano, Y., Iwasaki, S., Yoko, H., Udagawa, T., Li, S., Saeki, Y., Yoshihisa, T., Tanaka, K., et al. (2020). Ribosomal protein S7 ubiquitination during ER stress in yeast is associated with selective mRNA translation and stress outcome. Sci. Rep. *10*, 19669. https://doi.org/10.1038/s41598-020-76239-3.

70. Truitt, M.L., and Ruggero, D. (2016). New frontiers in translational control of the cancer genome. Nat. Rev. Cancer *16*, 288–304. https://doi.org/10.1038/nrc.2016.27.

71. Wang, D., Baumann, A., Szebeni, A., and Olson, M.O. (1994). The nucleic acid binding activity of nucleolar protein B23.1 resides in its carboxyl-terminal end. J. Biol. Chem. *269*, 30994–30998. https://doi.org/10.1016/s0021-9258(18)47380-2.

72. Pal, I., Safari, M., Jovanovic, M., Bates, S.E., and Deng, C. (2019). Targeting translation of mRNA as a therapeutic strategy in cancer. Curr. Hematol. Malig. Rep. *14*, 219–227. https://doi.org/10.1007/s11899-019-00530-y.